Supplementary information to Golini et al.

Figure S1

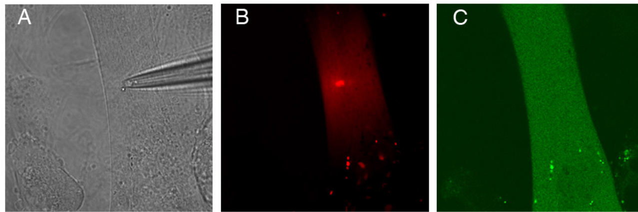

Figure S1. Rhod-2 Ca^{2+} measurements in myotubes. (x,y) images showing a pJPA-positive (green fluorescence) myotube whole-cell-clamped with a patch pipette containing the calcium-sensitive-dye rhod-2 (red fluorescence image). Image side size: 102 µm

Figure S2

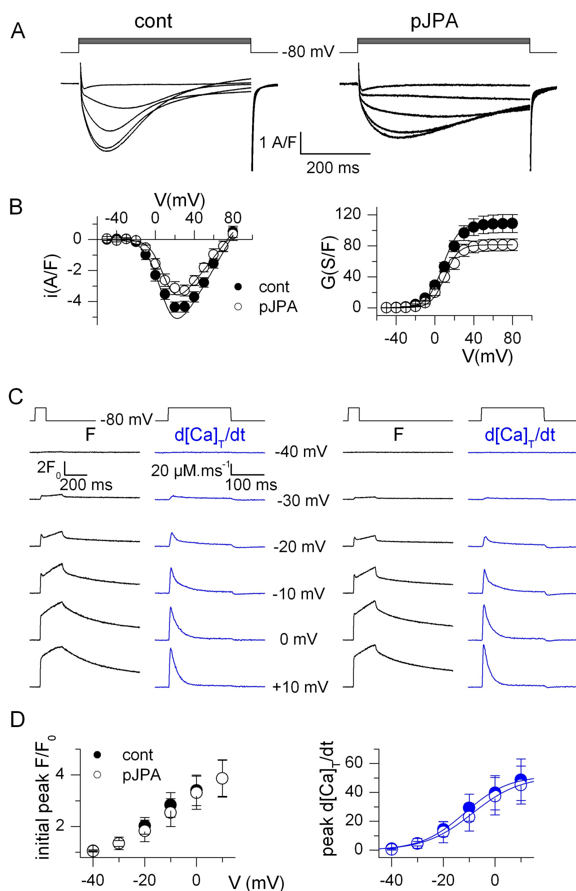

Figure S2. Voltage dependence of DHPR-mediated Ca^{2+} entry and Ca^{2+} release in control and JPs knockdown-positive adult muscle fibers. *A*, Ca^{2+} current traces obtained in a control (left) and in a pJPA-positive (right) muscle fiber in response to the depolarizing pulse protocol shown above; the current was measured in response to pulses from -80 mV to values ranging between -10 and +30 mV with a 10 mV increment. *B*, mean voltage dependence of the peak Ca^{2+} current density (left) and corresponding mean maximum conductance (right) in control (n=13) and pJPA-positive (n=14) muscle fibers. Superimposed lines were calculated from the average values of the parameters obtained from fitting the appropriate function to the individual series of data (see Methods). There was a slight

reduction of the L-type Ca^{2+} current density, corresponding to an ~25 % reduction of the peak conductance. Fitting the voltage dependence of the peak current in each cell gave mean values for G_{max}, V_{rev}, $V_{0.5}$ and k of 109 ± 11 S/F, 77.3 ± 3.7 mV, 8.3 ± 2.7 mV and 8.1 ± 0.6 mV in control fibers and of 81.5 ± 8 S/F, 74.3 ± 5.6 mV, 10.3 ± 2.4 mV and 7.0 ± 0.5 mV in pSuperJPAi-GFP-positive fibers, respectively. The mean maximum conductance value was significantly depressed in the pSuperJPAi-GFP-positive cells (P=0.04). *C*, rhod-2 fluorescence transients and corresponding Ca^{2+} release flux (blue traces, shown on an expanded time scale) from a control (left) and from a pJPA-positive (right) muscle fiber in response to depolarizing steps to the indicated levels. Rhod-2 signals were from spatially averaged confocal line-scan images. The Ca^{2+} release flux was estimated using a model of intracellular distribution that included EGTA as a major contributor to Ca^{2+} buffering (see SI Methods). There was no obvious qualitative difference between the control and the pSuperJPAi-GFP-positive fiber. *D*, voltage dependence of the mean initial peak amplitude of the rhod-2 transient (left) and of the peak Ca^{2+} release flux (right). A Boltzmann function was fitted to the two series of mean values of peak Ca^{2+} release, the result of which is shown as superimposed curves. The two sets of values did not differ.